

Investigation of four rotating radio transients properties at 111 MHz

S. A. Tyul'bashev^{1*} T. V. Smirnova¹ E.A.Brylyakova^{1,2} and M.A. Kitaeva¹

¹ *P.N. Lebedev Physical Institute of the Russian Academy of Sciences, Astro Space Center, Pushchino Radio Astronomy Observatory Radiotelescopnaya 1, Moscow reg., Pushchino, 142290, Russia*

² *P.N. Lebedev Physical Institute of the Russian Academy of Sciences Leninskii pr. 53, Moscow, 119991 Russia*

Accepted XXX. Received YYY; in original form ZZZ

ABSTRACT

The analysis of individual pulses of four rotating radio transients (RRATs), previously discovered in a monitoring survey running for 5.5 years at the frequency of 111 MHz, is presented. At a time interval equivalent to five days of continuous observations for each RRAT, 90, 389, 206, and 157 pulses were detected in J0640+07, J1005+30, J1132+25, and J1336+33, respectively. The investigated RRATs have a different distribution of the pulses amplitude. For J0640+07 and J1132+25, the distribution is described by a single exponent over the entire range of flux densities. For J1005+30 and J1336+33, it is a lognormal function with a power law tail. For J0640+07 and J1005+30, we have detected pulses with a signal-to-noise (S/N) ratio of few hundreds. For J1132+25 and J1336+33, the S/N of the strongest pulses reaches several tens. These RRATs show strong changing of character of emission. When strengths of pulse amplitudes significantly changed, we see long intervals of absence of emission or its strong attenuation. The analysis carried out in this work shows that it is possible that all the studied RRATs are, apparently, pulsars with giant pulses.

Key words: pulsars: general

1 INTRODUCTION

Rotating radio transients (RRATs) were discovered in 2006 (McLaughlin et al., 2006) as sources of sporadic bursts of dispersed pulses followed by no detectable emission for many rotations (sometimes minutes to hours) (Keane, 2016; Bhattacharyya et al., 2018). They are Galactic neutron stars with extreme emission variability. Single pulse rates are in the range of a few pulses to a few hundred pulses per hour. The nulling fraction of RRATs can exceed 99 percent. The average magnetic fields of RRATs and the average periods are higher than those of ordinary second pulsars (McLaughlin et al., 2009; Cui et al., 2017). Other qualities of RRATs are similar to those of pulsars with similar periods. According to the paper Burke-Spolaor (2010) Galactic z-distribution and pulse width distributions are the same as for ordinary pulsars.

Long-term studies of RRATs are still limited (Palliyaguru et al., 2011, Bhattacharyya et al., 2018, Mickaliger, 2018, Shapiro-Albert, 2018, Brylyakova, 2020). The authors of the paper Palliyaguru et al. (2011), Cui et al. (2017) analyzed the short and long-term variability of eight RRATs studied over a 5.5-year interval at frequency 1400 MHz. The paper shows that there are periodicities from 30 minutes to years in pulse arrival time for six investigated

RRATs and RRAT pulses appear randomly at small time intervals.

In the paper Cui et al. (2017) for eight RRATs, a series of observations from 1.5 to 15 years were used to obtain accurate estimates of the rotational parameters, as well as to obtain histograms of the pulses amplitude distributions. It turned out that the typical pulse distribution is lognormal, as for ordinary pulsars. A power law tail in the pulses energy distributions typical for pulsars with giant pulses have observed for several RRATs. Results of research on the pulses distribution by energy in the paper Mickaliger (2018) are the same as in Cui et al. (2017), but for 14 RRATs. A study of three RRATs over an eleven-year series of observations was presented in Shapiro-Albert, (2018). It shows that the energy distribution for two RRATs is lognormal, and for one, it is lognormal, and an additional a power component is observed.

Using simultaneous observation of single pulses of RRAT J2325-0530 at Murchison Widefield Array (MWA, 154 MHz) and Parkes radio telescopes (1.4 GHz) Meyers (2019) measure the spectral index $\alpha = 2.2 \pm 0.1$. Shapiro-Albert (2018) provided single-pulse based spectral index (α) for three studied RRATs which are between 0.6 and 1.2. Taylor (2016) measure α about 0.7 across band of LWA1 (35 - 80 MHz) for RRAT J2325-0530 which is substantially shallow than in Meyers (2019). It is possible that a flattening may occur at $f < 150$ MHz.

The eight-year observations for three RRATs are consid-

* E-mail: serg@prao.ru

ered in [Bhattacharyya et al. \(2018\)](#). It is shown in this paper that there may be long-term trends of changes in the observed arrival rate of pulses. The average number of observed pulses varies 1.5-2 times both in the direction of decreasing and increasing of the number of observed pulses over the full observation interval. It is noted in this paper that in the absence of strong pulses, one from investigated RRATs shows weak periodic emission.

The five-year observation interval at the frequency 111 MHz have used to study the RRAT J0139+33 ([Brylyakova, 2020](#)). We have shown that the energy distribution of pulses in the RRATs is described by bimodal (broken) power law, which is typical for some pulsars with giant pulses ([Smirnova, 2012](#), [Kazantsev, 2017](#)).

Summarizing the above mentioned observations, we can come to conclusion that the number of observed pulses can significantly change for RRAT at certain time intervals, trends can be observed that show an increase or decrease in the number of observed pulses over the entire observation interval. The pulse energy distribution function is usually log-normal, although a power law tail is sometimes observed. There is also one case of a broken power law distribution.

In 2018, when processing semi-annual daily observations obtained at the Large Phased Array (LPA) radio telescope of the Lebedev Physical Institute (LPI), 33 RRATs were detected by their individual dispersed pulses ([Tyulbashev, 2018](#), [Tyulbashev, 2018a](#)). Out of this sample, we have selected for further studies four RRATs that have long nullings or strong individual pulses. These RRATs were discovered in the monitoring survey carried out at the LPA LPI at a wavelength of 2.7 meters. They have not yet been confirmed by observations on other instruments. In particular, they were not detected in the search for pulsars on LOFAR ([Sanidas, 2019](#)) at the wave length 2.2 m.

2 OBSERVATIONS

Round-the-clock daily monitoring observations were carried out on the upgraded antenna of the LPA LPI since August 2014. LPA LPI consists from 16384 wave dipoles. These are 256 lines each of which has 64 dipoles. We have used Butler matrices to form a beams in the Meridian plane. Details about the modernization of the LPA LPI are given by [Shishov \(2016\)](#) and [Tyulbashev \(2016\)](#).

The main purpose of the monitoring program is daily observations under the 'Space Weather' program. In this program, daily observations of about 5000 compact (scintillating) radio sources are carried out ([Shishov, 2016](#)). Observations made for the 'Space Weather' program can also be used to study pulse emission ([Brylyakova, 2020](#)).

The antenna operates at a central frequency of 110.3 MHz. The full band 2.5 MHz is divided into 32 frequency channels with a channel width of 78 kHz. The sampling interval is equal to 12.5 ms. Observations are done simultaneously in 96 antenna beams covering declinations from -9° to $+42^\circ$. The data obtained are used to search for new RRATs and pulsars.

Digital recorders were created for these observations do not allow us to get more frequency channels and readout time less than 12.5 ms. The accuracy of the timestamps are determined by the quartz oscillator. Therefore raw data are not optimal for pulsar and RRAT investigations.

Six times a day a signal of known temperature (calibration signal) is applied to the antenna input in the form of "OFF-ON-OFF", this allows to equalize the gain between frequency channels ([Tyulbashev, 2020](#)). As the data analysis showed, during a 2-hour observation, the change in the calibration signal amplitude does not exceed 5%. Since the closest calibration signal to the source is used for session calibration, the detected pulse amplitudes have errors of less than 5%. The width of beam directivity pattern of the LPA LPI at half power is equal to $3.5 \text{ minutes} / \cos(\delta)$ (δ is a source declination).

The typical sensitivity of the LPA LPI telescope when observing ordinary pulsars in a single observation session is 6-8 mJy, if the pulsar is outside the plane of the Galaxy and 15-20 mJy, if the pulsar is in the plane of the Galaxy ([Tyulbashev, 2016](#)). The detection limit for single pulses with the selected sampling interval 12.5 ms is 2.1 Jy at S/N (signal to noise ratio) = 7 ([Tyulbashev, 2018](#)). For 5.5 years of continuous monitoring, the equivalent continuous observation time is approximately five days for each point in the sky that falls within the observation area.

Additional information about observation modes with LPA LPI, on implementation of independent radio telescopes based on a single antenna field and other technical information about the capabilities of the LPA LPI after its modernization can be found in the papers [Shishov \(2016\)](#), [Tyulbashev \(2016\)](#).

3 DATA ANALYSIS

LPA LPI have a lot of specifics as antenna array. Therefore, special software were created to process the observations, taking into account these features. We have hosted this software on Github¹.

We followed by standard way for search of RRAT pulses in the obtained data. After equalizing the amplification between the frequency channels, we incoherently dedispersed the data to the known dispersion measure (DM) of the studied RRATs, subtracted the baseline and removed radio frequency interference (RFI), and detected single pulse from the frequency averaged time series. Details of RFI removal are described in [Tyulbashev \(2020\)](#).

To get the baseline, a recording section containing a pulse and having a duration of four seconds was taken. This time interval is much longer than the duration of the RRAT pulse, which makes it possible to adequately determine the baseline ([Brylyakova, 2020](#)). First, the frequency channels were summed up without shifts, that is, assuming a DM is equal zero. The resulting points were fit by a polynomial. Then the frequency channels were summed up with shifts corresponding to the DM of the RRAT. The resulting polynomial was subtracted from the resulting series of points. The root-mean-square deviation (σ_n) of the noises was determined by the area outside the pulse and the S/N was taken as the value of the peak pulse amplitude divided by the estimate of σ_n (see details in the paper [Brylyakova \(2020\)](#)). For J1005+30, J1132+25 and J1336+33, the pulse detection threshold was set at S/N of 6. For J0640+07 the threshold was increased to

¹ https://github.com/Elinxt/rrat_pulsars

$S/N \geq 7$ since a lower threshold resulted in an overwhelming number of false positive detections.

For further work, pulses were selected that were located at an interval of ± 1.5 minutes from the pulsar passing through the center of the beam. For each pulse, corrections to the detected were made related to the features of LPA LPI, as an antenna array (Tyulbashev, 2016, Shishov, 2016). These corrections attempt to mitigate the fact that the direction of the formed radiation pattern does not coincide with the direction to the source (details see in Brylyakova (2020)). For all detected signals, the average profile and dynamic spectrum files were saved for each observation session. The final selection of pulses was done manually. The average profile was determined by summing up a signal with a given period, if it is known.

As a result of processing, data series were obtained in which the time of arrival of the RRAT pulse and its amplitude (I_k), normalized to the σ_n were recorded for each date over the entire observation interval. These series were analyzed to study time variations, the number of pulses, and their amplitudes. Since the data is calibrated based on the calibration signal, it reflects the correct distribution of amplitudes over a long time interval.

4 RESULTS

Figs 1 and 2 show the values of the amplitudes in units of S/N , and the number of recorded pulses per session for the selected objects, depending on the sequence of days starting from the first day indicated in Table 1.

Table 1 shows information about the observed pulses. In the first column, there is the name of the RRAT. Columns 2-3 show the period (P_1) and the dispersion measure of the RRAT, and columns 4-8 show the date when the first pulse was detected, total number of observation days between the first and last recorded pulse (N_{all}), number of detected pulses (N_p), the ratio of the number of days in which the pulses were detected to the number of all days of observation, i.e. intermittency factor (f_{int}), maximum continuous duration absence of pulses in days (N_{max}). Columns 9-12 show average values of amplitudes (in S/N units) for all detected pulses exceeding the specified threshold, $\langle I \rangle_1$, average values taking into account intermittency factor, $\langle I \rangle_2 = \langle I \rangle_1 \times f_{int}$, maximum value of S/N for the entire observation period, I_{max} , modulation index $m = \sum_{i=1}^N [(I_i - \langle I \rangle_1)^2 / (N-1)]^{1/2} / \langle I \rangle_1$, where N is the number of pulses, and I_i is the amplitude of pulse i .

The sources in Table 1 can be divided into two samples. In the first sample, there are sources with high modulation and relatively short intervals when no pulses were observed, in the second sample, there are sources with low modulation and intervals when pulses are not detected for many months.

4.1 J0640+07 and J1005+30 – RRATs with giant pulses?

Number of known pulsars with giant pulses (GP) very small compared to the nearly three thousand pulsars published in the ATNF² catalog. According to Table 1 (Kazantsev, 2018)

with citations of original discoveries of GP the number of such pulsars were sixteen. The original papers consider a number of features that distinguish pulsars with giant pulses from ordinary pulsars Sutton (1971), Kinkhabwala, (2000), Soglasnov, (2004), Hankins, (2007), Kazantsev (2018). If we consider the radio range, such features may be (Kazantsev (2018)): high peak flux densities in the pulse compared to the peak flux density accumulated in the average profile (the ratio more than thirty); the power law distribution of pulse energy; the narrowness of the giant pulse compared to the average profile, sometimes it is an extreme narrowness of the pulse; high degree of polarization; extremely high brightness temperatures for the narrowest (nanoseconds) pulses. However, not all of these features are simultaneously observed in every pulsar with giant pulses. The issue of the ratio of the amplitudes (or energies) of pulses and the average profile for determining the "gigantism" of pulses is also not strictly defined. So in the paper of Karuppusamy (2012), it is considered that for giant pulses, their energy must exceed the energy of the average pulse by more than 10 times.

From the set of listed "gigantism" features in our monitoring observations, we can check the distribution of pulses by amplitudes or by energies and determine the peak flux densities. It is also necessary to obtain the average profile of the pulsar and compare its amplitude with the amplitude of the strongest observed pulses. If the ratio of amplitudes is at least 30 and the ratio of energies is more than 10, then the studied pulsar is a candidate for pulsars with giant pulses. For RRATs J0640+07 and J1005+30, the period has not yet been determined. The average profile with the lack of timing and a small number of observed pulses per session (one or two) could not be obtained for either J0640+07 or J1005+30 and that's why the ratio of amplitudes was determined from the detected pulses as $I_{max}/\langle I \rangle_2$. As will be shown below, for J1132+25, J1336+33 the value $\langle I \rangle_2$, corresponds well enough to the amplitude of the average profile. This gives the reason to believe that also for the RRATs considered here, obtained value of $\langle I \rangle_2$ determines the amplitude of the average profile. As follows from Table 1, the ratio $I_{max}/\langle I \rangle_2$ is equal to 466 (J0640+07) and 62 (J1005+30) for the strongest pulses. Fig. 1 shows dependence of the signal amplitude in S/N units (top) and the number of registered pulses (bottom) vs. time in days. These amplitude ratios and their distribution functions (analysed in Section 4.3) are GP-like features.

The RRATs J0640+07 and J1005+30 are characterized by a high modulation index associated with strong deviations of the amplitude from the mean value. The emission of J0640+07 and J1005+30 is sporadic. For J0640+07, before the pulse with the maximum amplitude $S/N = 289$ (Fig.1, on the left), eight days before it and another 9 days after it not a single pulse was registered. In this session, it was also the only one. For J1005+30, on the days of the largest amplitudes (Fig. 1, on the right) no pulses above the threshold were registered for several days before it and after it. Figure 3 shows the strongest pulses for J0640+07 and J1005+30. The average rate of occurrence of pulses per observational session is 0.05 (J0640+07) and 0.20 (J1005+30). Average number of pulses during three minutes session of observation $N_p/(f_{int} \times N_{all})$ is equal to 1.05 and 1.06 if we registered pulses during sessions (Fig. 1, bottom).

² <https://www.atnf.csiro.au/people/pulsar/psrcat/>

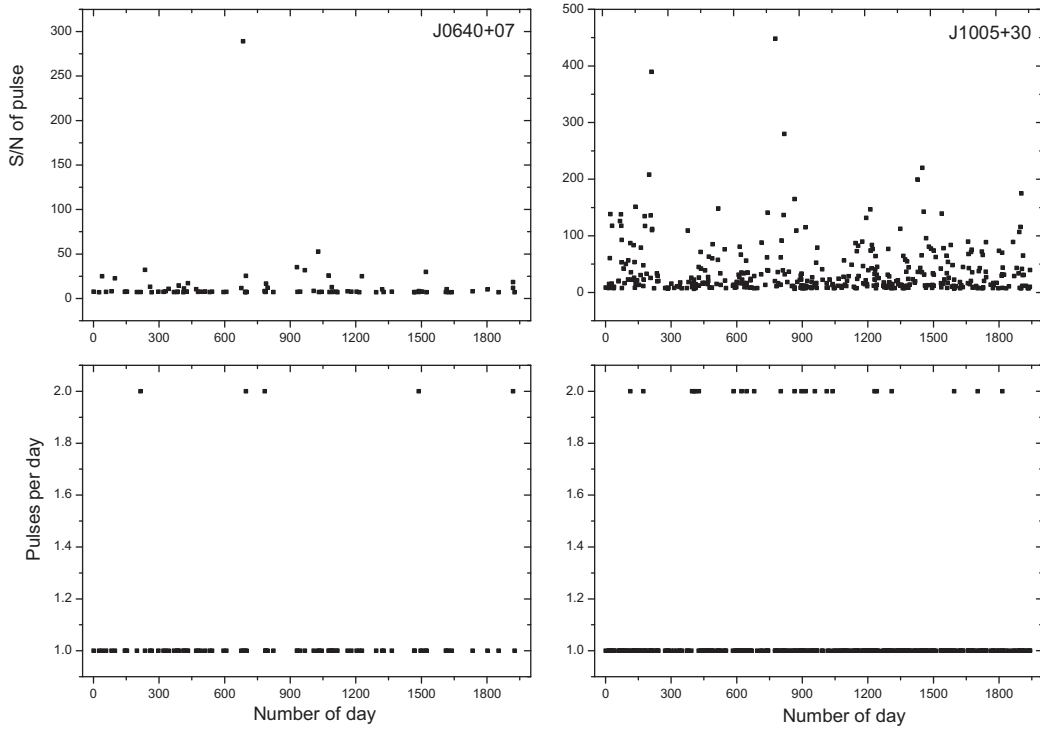


Figure 1. Vertical axis is the pulse amplitude in S/N units (top) and the number of registered pulses (bottom). Horizontal axis is defined as the number of the corresponding days. The first day with number 0 corresponds to $JD = 2456920$ for J0640+07 and $JD = 2456898$ for J1005+30.

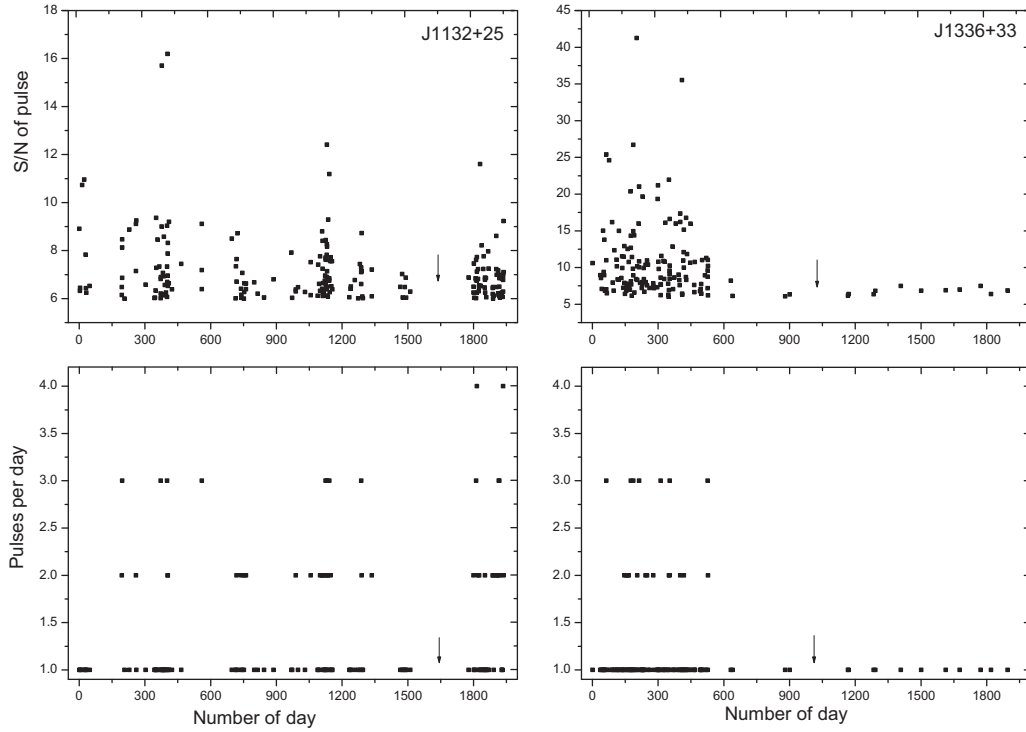


Figure 2. Horizontal and vertical axes are similar to the axes in Fig.1. The first day with number 0 corresponds to $JD = 2456896$ for J1132+25 and for J1336+33.

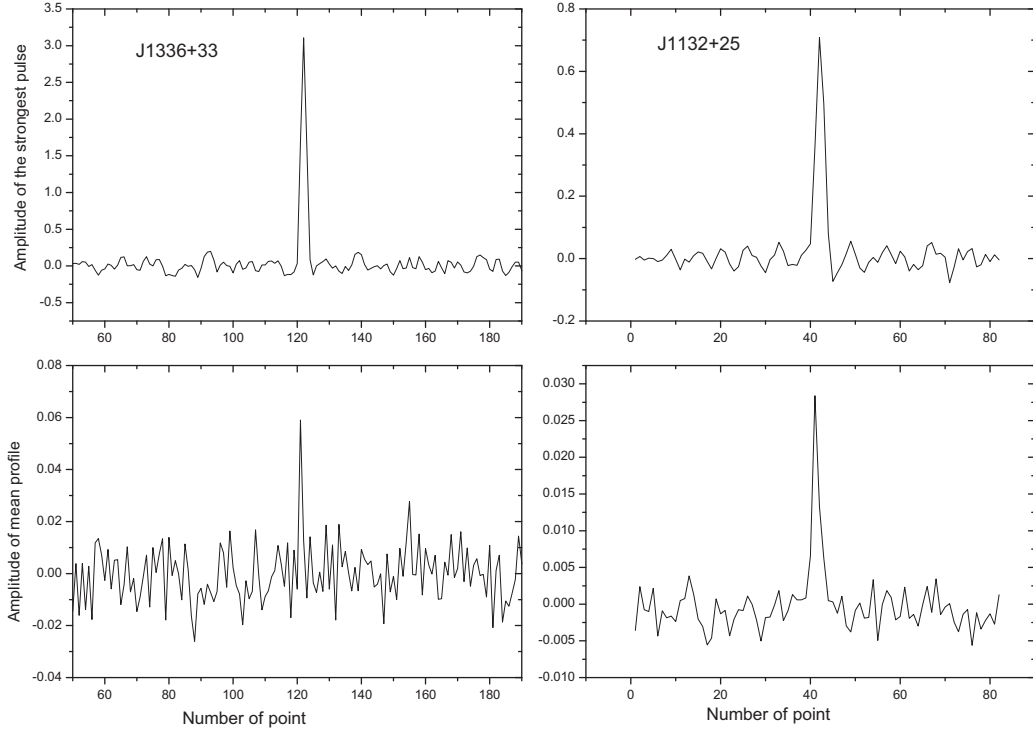


Figure 3. Vertical axis (amplitude) is shown in arbitrary units. Horizontal axis is a time in points ($\delta t = 12.5$ ms). The strongest pulses J1132+25 (top, right) and J1336+33 (top, left) and the average profiles of these RRATs (bottom).

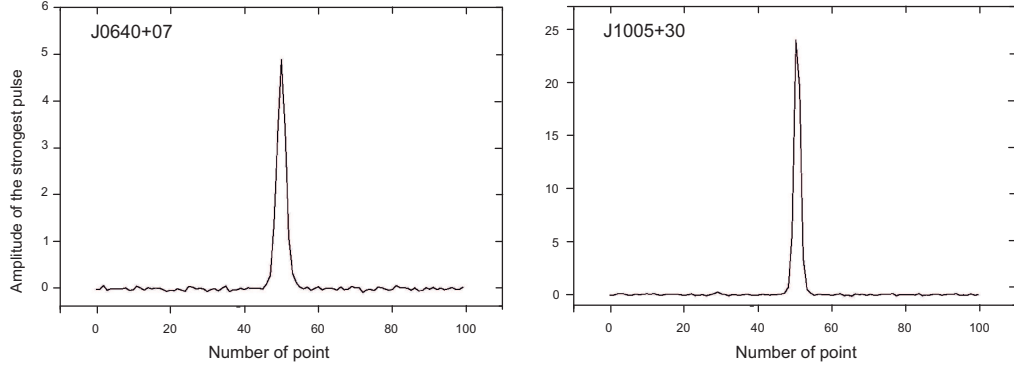


Figure 4. Vertical axis (amplitude) is shown in arbitrary units. Horizontal axis is a time in points ($\delta t = 12.5$ ms). The strongest pulses for J0640+07 (left) and J1005+30 (right).

Table 1. Summary of recorded pulses data.

PSR	P_1 (s)	DM (pc/cm ³)	First date	N_{all} (days)	N_p	f_{int}	N_{max} (days)	$\langle I \rangle_1$	$\langle I \rangle_2$	I_{max}	m
J0640+07	-	52	19 Sept. 2014	1927	90	0.044	107	14	0.62	289	2.2
J1005+30	-	17.5	24 Sept. 2014	1942	389	0.188	31	38.3	7.2	448	1.25
J1132+25	1.002	23	26 Aug. 2014	1937	206	0.075	265	7.13	0.53	16.2	0.2
J1336+33	3.013	8.5	26 Aug. 2014	1896	157	0.069	256	10.4	0.71	41.3	0.5

4.2 J1132+25 and J1336+33 – highly intermittent RRATs

RRATs J1132+25 and J1336+33 differ from RRATs J0640+07 and J1005+30. They have a sharp change in amplitudes, accompanied by the absence of emission or its sharp weakening for a long time like intermittent pulsars. For RRAT J1132+25 there is long continuous time intervals (of 265 ses-

sions, marked by arrows in Fig. 2), when there are no pulses exceeding the specified threshold. The same figure also shows the highly sporadic nature of these RRATs emission, when long periods of quiescence are replaced by a significant increase in both the amplitude and the number of observed pulses. It turned out that, as for J0640+07 and J1005+30,

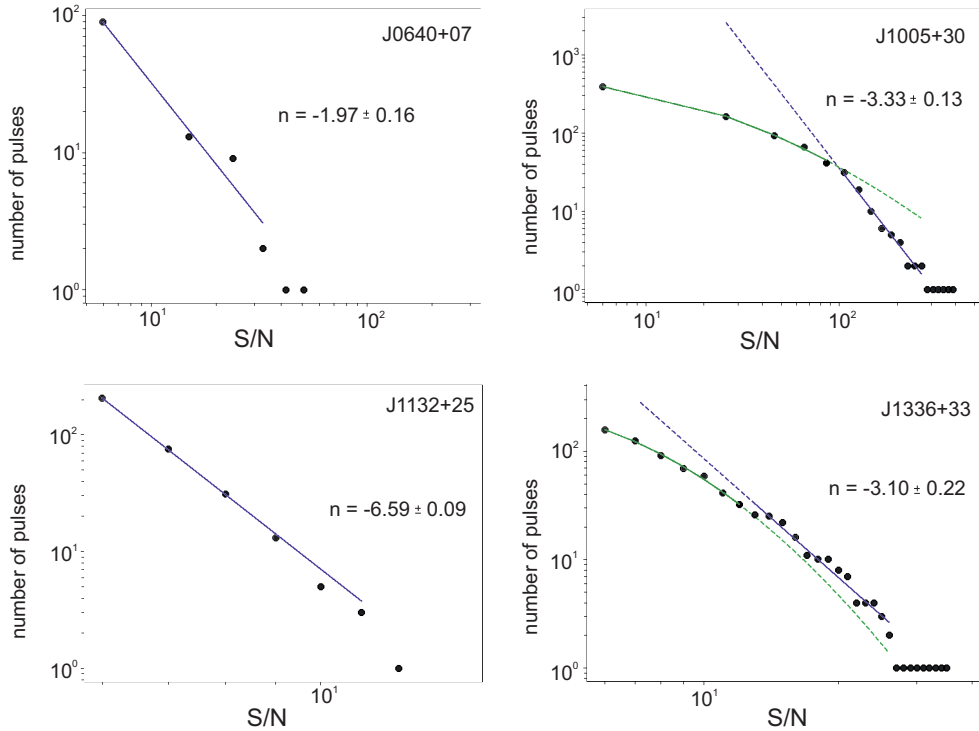


Figure 5. Integral distribution functions of the number of pulses (vertical axis) vs. the pulse amplitude in S/N units (horizontal axis) in a logarithmic scale. The data points are approximated by different laws (see Table 2) using the least squares method. Obtained power coefficients n with their errors are indicated in the figure.

they have features of giant pulses: $I_{max}/\langle I \rangle_2 = 30.4$ for J1132+25 and $I_{max}/\langle I \rangle_2 = 57.9$ for J1336+33.

In contrast to RRATs J0640+07 and J1005+30, for which we were not able to obtain average profiles, for J1132+25, J1336+33, the usual pulsar type periodic emission was detected previously (the periods shown in Table 1 obtained in the paper Tyulbashev (2018a)). Their average profiles and the strongest pulses are shown in Fig. 4. When obtaining average profiles, at least twenty sessions were randomly selected for each source, during which no strong pulses were observed to exclude influence of them on the profile. For these days, average profiles were obtained after averaging the signal with a known period. It is indicated that weak emission exist even we do not see strong pulses. Since the individual strong pulses and the resulting average profiles were normalized by the calibration signal, it is possible to determine the ratio of the amplitude in the pulse to the amplitude of the average profile.

As can be seen from Fig. 4, the width of the individual pulse and of the average profile at the FWHM level for J1132+25 and J1336+33 are comparable, and the pulse shapes are similar, so we can assume that the ratio of their amplitudes corresponds to the ratio of their energies. We calculated energies as the integral over the pulse or average profile up to the 6 sigma noise level. Using the obtained shapes of the profile and of individual pulse, we obtained the ratio of the energy in the pulse to the energy of the average profile: $E = E_{pulse}/E_{profile}$. These values for the strongest pulses are equal to: $E = 25.3$ (J1132+25), $E = 50.1$ (J1336+33). We note that these energies are close (the difference is of the order of 10%) to the quantity $I_{max}/\langle I \rangle_2$, and so we can assume that $\langle I \rangle_2$ approximates the amplitude of the average profile. These ratios of

the energy in the pulse to the energy of the average profile and also the amplitude distribution analysed in Section 4.3 tell us that RRATs could be GP emitters.

The average profiles of pulsars J1132+25 and J1336+33, obtained at a three-minute interval and then averaged over several sessions, perhaps do not reflect the real average profile, which should be determined on at least half an hour interval. In addition, the average profile we use is affected by polarization, since the antenna receives linearly polarized emission, and if the period of the Faraday rotation of the polarization plane is comparable to or longer than the receiver band, then the amplitude of such a profile can vary by several times from session to session. Such behavior shows PSR B0950+08 (Smirnova, 2012) observed at 112 MHz. This pulsar has about 70 % linear polarization of emission and 15 MHz period of the Faraday rotation which considerably exceeds the receiver bandwidth. This pulsar has one of the smallest rotation measure ($RM = 1.35 rad/m^2$) and so the largest profile amplitude instability from session to session compare to other pulsars. Polarization study of 22 known RRATs by Caleb (2019) with the Parkes telescope had shown that average linear polarization fraction of 40 per cent. Individual single pulses were observed to be up to 100 per cent linearly polarized. At our low frequency the level of polarization can be about this value. However the value $\langle I \rangle_2$ obtained from many pulses will correctly reflect the amplitude of the average profile.

An influence of diffraction scintillations on the profile is very small in our case, since the de-correlation bandwidth for the selected RRATs, according to our estimates (less than a few kHz), is significantly narrower than the receiver band (2.5 MHz). Refractive scintillations for selected objects at our

frequency have a scale of the order of a year or longer, so they also do not affect the value of the average profile amplitude. Our estimation of the diffractive scintillation bandwidths f_{dif} and the time scale of refractive scintillation is based on the YMW16 Galactic electron density distribution model (Yao, 2017). Our measurements are in agreement with previous low-frequency estimates from low-DM pulsars (Malofeev, 1995).

For these two sources, as well as for J0640+07 and J1005+30, we have a small value of the ratio of the number of days in which pulses were detected to the total number of all observation days: $f_{int} = 0.075$ and 0.069 , as well as a small number of pulses exceeding the threshold in the observation session. The average rate of occurrence of pulses per minute is 0.037 (J1132+25) and 0.027 (J1336+33). Average number of pulses per minute is equal to 0.47 (J1132+25) and 0.4 (J1336+33) if we registered pulses during sessions (Fig. 2, bottom).

The modulation index for J1132+25 and J1336+33 is smaller than 1. As can be seen from Fig. 2, the emission has the flashy character, when the signal amplitude changes dramatically. Especially strong is the change in amplitude for J1336+33, when, after 524 days of high activity, only weak and single pulses are recorded with large intervals of their complete absence (265 and 256 days) up to the last day of observations.

4.3 Distribution function of pulses

The number of detected pulses in the studied RRATs is low. Early observations of four RRATs (McLaughlin et al., 2006) with a small number of detected pulses (from 11 to 229) showed a power-law distribution of the pulses over the amplitudes. In the paper Mickaliger (2018), the dependencies of the same RRATs are shown by the sum of two lognormal distributions.

We checked different fits in the resulting histograms: power law, broken power law, lognormal distribution, lognormal distribution with a power tail.

$$f(x) = q/x \cdot e^{-(\ln(x)-w)^2/2c^2}$$

$$f(x) = a \cdot x^b,$$

where q , w , c , a , b are fitting parameters of lognormal and power law distributions.

For the fitting, we used the Levenberg-Marquardt non-linear least squares method (see library of Python: LMFIT). Table 2 contains results of model testing using the Akaike information criterion (AIC³) corrected for small sample size (AICc, see details in Burnham (2002)). Bold text in the table indicates the best fit, which corresponds to the lowest number in the Table 2 for different models.

For RRAT J0640+07, the number of detected pulses is less than one hundred. Therefore, there are no pulses in the majority of the defined S/N bins. We have increased the size of the bin by nine times, to build a smoothed distribution.

In Fig. 5 integral distribution functions are given for all four sources in a logarithmic scale. It is clear that J0640+07

and J1132+25 have a power law spectrum. J1005+30 (up to $S/N = 72$) and J1336+33 (up to $S/N = 12$) have a lognormal distribution and the power law distribution above these S/N.

Power or power tail dependencies for distribution functions are additional indirect signs of pulsars with giant pulses. However, the small number of detected pulses does not give us complete confidence to say that investigated RRATs are a pulsar with giant pulses.

5 DISCUSSION

All four RRATs have a number of common features: 1) flashy character when the amplitude of the signal increases by several times compared with adjacent sessions (for J1132+25) and even 1-2 orders of magnitude (for J0640+07, J1005+30, J1336+33); 2) a large number of days when there are no pulses above the specified detection threshold (long quiescence periods): $f_{int} < 0.2$; 3) a significant predominance of sessions with only one pulse for 3 minutes of the source passing through the beam of the LPA LPI at half power; 4) the maximum number of pulses registered per three minutes does not exceed four (J1132+25, J1336+33), and even two (J0640+07, J1005+30); 5) power law (J0640+07, J1132+25), and lognormal with a power law tail (J1005+30, J1336+33) distribution of pulse amplitudes; 6) the excess of peak amplitudes and energies by tens and hundreds of times relative to the corresponding values for the average profiles, which is typical for pulsars with giant pulses.

The strongest change in activity was observed for J1336+33. For 524 days, it showed high activity when S/N was up to 41, and then for 1372 days, only solitary weak (at the detection level) pulses were observed with long time intervals between them. It is also possible that nulling is characterized by very weak emission and the sensitivity of the LPA LPI is not enough to detect it. Anyway, J1336+33 is significantly distinguished from all known RRATs by rapid changing of activity to long interval of (around three years) absence of emission or its strong attenuation. It would be interesting to study this object using timing to see if this rapid changing is caused by changing of period and period derivative. Unfortunately we did not have this possibility. Although the observation session lasts only three minutes, however, the appearance of single pulses is a random process and the absence of pulses over a long time interval during daily observation of sources could reflect a systematic and persistent change in the emission process.

The modulation index reflects amplitude variability in time and it is significantly different for J0640+07, J1005+30 ($m = 2.2$ and 1.25) and 1132+25, 1336+33 ($m = 0.2$ and 0.5). In this case, a small value of m is caused mainly by long intervals of nulling or strong decreasing of emission. For RRATs J0640+07, J1005+30 we have rare pulses but they are more smoothly distributed in time (see Fig. 1) and the ratio of the amplitude of the strongest pulse to the mean amplitude $I_{max}/\langle I_2 \rangle$ for them is much larger than for another two pulsars. Both of these qualities collectively lead to $m > 1$.

A strong change in the character of emission can be associated with both external and internal causes. RRATs can be extinct pulsars that are re-activated due to the interaction of the pulsar's magnetosphere with the matter falling onto it, or the interaction of the magnetosphere with the surround-

³ <https://github.com/lmfit/lmfit-py/>

Table 2. Tests of different laws of pulse amplitude distribution. The values in the Table correspond to the AICc score for each model per pulsar.

RRAT name	power	broken power	lognormal + power tail	lognormal
J0640+07	9	36	39	53
J1005+30	85	62	16	49
J1132+25	5	14	30	21
J1336+33	65	51	31	37

ing matter (Li et al., 2006, Luo & Melrose, 2007). Internal causes can be determined by a sharp change in the primary plasma density or the conditions of emission propagation in the magnetosphere (Timokhin, 2010).

The broken power law character of the distribution was previously obtained for RRAT J0139+33 (Brylyakova, 2020), which was also observed at the frequency of 111 MHz. This distribution pattern is one of the main features of giant pulses. In the paper of Karuppusamy (2012) giant pulses are defined as pulses with an energy exceeding the energy of the average profile by more than 10 times. This ratio is quite arbitrary, and the RRATs for which the average profile was obtained (J1132+25, J1336+33) satisfy this condition. Studies at higher frequencies: 1400 and 820 MHz (Cui et al., 2017, Mickaliger, 2018) had shown that for most RRATs the distribution of amplitudes and energies is mostly lognormal, as for ordinary pulsars, but a few RRATs had a log-normal distribution with a power law tail.

There is only one investigation with simultaneous observations RRAT at meter and decimeter wavelength (Meyers, 2019). They find that the single-pulse amplitude distribution is a truncated exponential at 150 MHz and a power law at 1400 MHz.

Other studies of the pulse amplitude distribution in more than two dozen RRATs discovered in the decimeter wavelength range (Cui et al., 2017, Mickaliger, 2018, Shapiro-Albert, 2018) showed a lognormal or lognormal with power law tail distribution. Meyers (2019) estimated the pulse energy distribution for J2325-0530 at 150 MHz and 1400 MHz but because of small sample of single pulses they were unable to draw concrete conclusions. Since our sample is small and does not have observations at higher frequencies, it is impossible to conclude that the distribution of the pulse amplitude may depend on the frequency of observations for all RRATs. The analysis shows that RRATs are not a homogeneous sample, but a mixture of different kinds of pulsars, and long-term studies of large RRATs samples are needed, which will allow us to judge more accurately the validity of different hypotheses.

6 DATA AVAILABILITY

The raw data underlying this article will be shared on reasonable request to the corresponding author. The tables with S/N of pulses are in <http://prao.ru/online%20data/online%20data.html>

ACKNOWLEDGEMENTS

The PYTHON LMFIT package⁴ was used for data analysis. The authors express their appreciation to V.M.Malofeev, V.A. Potapov, A.N.Kazantsev for useful discussions in the course of the work. Special thanks to Yu.Yu. Kovalev for a donated server that was used to process observations data.

REFERENCES

- Bhattacharyya, B., Lyne, A. G., Stappers, B. W., Weltevredre, P., Keane, E. F., McLaughlin, M. A., Kramer, M., Jordan, C., Bassa, C. 2018. A long-term study of three rotating radio transients. *Monthly Notices of the Royal Astronomical Society* 477, 4090.
doi: 10.1093/mnras/sty923
- McLaughlin, M. A., Lyne, A. G., Lorimer, D. R., Kramer, M., Faulkner, A. J., Manchester, R. N., Cordes, J. M., Camilo, F., Possenti, A., Stairs, I. H., Hobbs, G., D'Amico, N., Burgay, M., O'Brien, J. T. 2006. Transient radio bursts from rotating neutron stars. *Nature* 439, 817.
doi: 10.1038/nature04440
- McLaughlin, M. A., Lyne, A. G., Keane, E. F., Kramer, M., Miller, J. J., Lorimer, D. R., Manchester, R. N., Camilo, F., Stairs, I. H. 2009. Timing observations of rotating radio transients. *Monthly Notices of the Royal Astronomical Society* 400, 1431.
doi: 10.1111/j.1365-2966.2009.15584.x
- Li, Xiang-Dong. 2006. On the Nature of Part-Time Radio Pulsars. *Astrophysical Journal Letters* 646, L139.
doi: 10.1086/506962
- Luo, Q., Melrose, D. 2007. Pulsar radiation belts and transient radio emission. *Monthly Notices of the Royal Astronomical Society* 378, 1481.
doi: 10.1111/j.1365-2966.2007.11889.x
- Palliyaguru, N. T., McLaughlin, M. A., Keane, E. F., Kramer, M., Lyne, A. G., Lorimer, D. R., Manchester, R. N., Camilo, F., Stairs, I. H. 2011. Radio properties of rotating radio transients - I. Searches for periodicities and randomness in pulse arrival times. *Monthly Notices of the Royal Astronomical Society* 417, 1871.
doi: 10.1111/j.1365-2966.2011.19388.x
- Cui, B. Y., Boyles, J., McLaughlin, M. A., Palliyaguru, N. 2017. Timing Solution and Single-pulse Properties for Eight Rotating Radio Transients. *Astrophysical Journal* 840, 5.
doi: 10.3847/1538-4357/aa6aa9
- Mickaliger, Mitchell B., McEwen, A. E., McLaughlin, M. A., Lorimer, D. R. 2018. A study of single pulses in the Parkes Multibeam Pulsar Survey. *Monthly Notices of the Royal Astronomical Society* 479, 5413.
doi: 10.1093/mnras/sty1785

⁴ <https://zenodo.org/record/4516651>

- Shapiro-Albert, B. J., McLaughlin, M. A., Keane, E. F. 2018. Radio Properties of Rotating Radio Transients: Single-pulse Spectral and Wait-time Analyses. *Astrophysical Journal* 866, 152. doi: 10.3847/1538-4357/aae2b2
- Brylyakova, E. A., Tyul'bashev, S. A. 2020. Investigation of RRAT J0139+33 at the Frequency of 111 MHz. *Astronomy and Astrophysics* in press. doi: 10.26119/978-5-6045062-0-2_2020_443
- Tyul'bashev, S. A., Tyul'bashev, V. S., Malofeev, V. M., Logvinenko, S. V., Oreshko, V. V., Dagkesamanskii, R. D., Chashei, I. V., Shishov, V. I., Bursov, N. N. 2018. Detection of Five New RRATs at 111 MHz. *Astronomy Reports* 62,63. doi: 10.1134/S1063772918010079
- Tyul'bashev, S. A., Tyul'bashev, V. S., Malofeev, V. M. 2018. Detection of 25 new rotating radio transients at 111 MHz. *Astronomy and Astrophysics* 618, A70. doi: 10.1051/0004-6361/201833102
- Tyul'bashev, S. A., Tyul'bashev, V. S., Oreshko, V. V., Logvinenko, S. V. 2016. Detection of new pulsars at 111 MHz. *Astronomy Reports* 60,220. doi: 10.1134/S1063772916020128
- Shishov, V. I., Chashei, I. V., Oreshko, V. V., Logvinenko, S. V., Tyul'bashev, S. A., Subaev, I. A., Svidskii, P. M., Lapshin, V. B., Dagkesamanskii, R. D. 2016. Monitoring of the turbulent solar wind with the upgraded Large Phased Array of the Lebedev Institute of Physics: First results. *Astronomy Reports* 60,1067. doi: 10.1134/S1063772916110068
- Tyul'bashev, S. A., Kitaeva, M. A., Tyul'bashev, V. S., Malofeev, V. M., Tyul'basheva, G. E. 2020. Detection of Five New Pulsars with the BSA LPI Radio Telescope. *Astronomy Reports* 64, 526. doi: 10.1134/S1063772920060074
- Burke-Spolaor, S., Bailes, M. 2010. The millisecond radio sky: transients from a blind single-pulse search. *Monthly Notices of the Royal Astronomical Society* 402,855. doi: 10.1111/j.1365-2966.2009.15965.x
- Taylor, G. B., Stovall, K., McCrackan, M., McLaughlin, M. A., Miller, R., Karako-Argaman, C., Dowell, J., Schinzel, F. K. 2016. Observations of Rotating Radio Transients with the First Station of the Long Wavelength Array. *Astrophysical Journal* 831, 140. doi: 10.3847/0004-637X/831/2/140
- Smirnova, T. V. 2012. Giant pulses from the pulsar PSR B0950+08. *Astronomy Reports* 56, 430. doi: 10.1134/S106377291205006X
- Kazantsev, A.N., Potapov, V.A. 2017. Observations of giant pulses from B1237+25 (J1239+2453) at 111 MHz. Detection and classification. *Astronomy Reports* 61, 747.
- Kazantsev, A.N., Potapov, V.A. 2018. Search for giant pulses of radio pulsars at frequency 111 MHz with LPA radio telescope. *Research in Astronomy and Astrophysics* 18, 8, 097. doi: 10.1088/1674-4527/18/8/97
- Sutton, J.M. and Staelin, D.H. and Price, R.M. 1971. Individual Radio Pulses from NP 0531. The Crab Nebula. *IAU Symposium* 46, 97.
- Kinkhabwala, A., Thorsett, S. E. 2000. Multifrequency Observations of Giant Radio Pulses from the Millisecond Pulsar B1937+21. *Astrophysical Journal* 535, 365. doi: 10.1086/308844
- Soglasnov, V. A., Popov, M. V., Bartel, N., Cannon, W., Novikov, A. Yu., Kondratiev, V. I., Altunin, V. I. 2004. Giant Pulses from PSR B1937+21 with Widths ≤ 15 Nanoseconds and $T_b \geq 5 \times 10^{39}$ K, the Highest Brightness Temperature Observed in the Universe. *Astrophysical Journal* 616, 439. doi: 10.1086/424908
- Hankins, T.H., Eilek, J.A. 2007. Radio Emission Signatures in the Crab Pulsa. *Astrophysical Journal* 670, 693.
- Karuppusamy, R., Stappers, B. W., Lee, K. J. 2012. Crab giant pulses at low frequencies. *Astronomy and Astrophysics* 538, 7. doi: 10.1051/0004-6361/201117667
- Sanidas, S., Cooper, S., Bassa, C. G., Hessels, J. W. T., Kondratiev, V. I., Michilli, D., Stappers, B. W., Tan, C. M., van Leeuwen, J., Cerrigone, L., Fallows, R. A., Iacobelli, M., Orrú, E., Pizzo, R. F., Shulevski, A., Toribio, M. C., ter Veen, S., Zucca, P., Bondonneau, L., Griebmeier, J. -M., Karastergiou, A., Kramer, M., Sobey, C. 2019. The LOFAR Tied-Array All-Sky Survey (LOTAAS): Survey overview and initial pulsar discoveries. *Astronomy and Astrophysics* 626, 104. doi: 10.1051/0004-6361/201935609
- Meyers, B. W., Tremblay, S. E., Bhat, N. D. R., Shannon, R. M., Ord, S. M., Sobey, C., Johnston-Hollitt, M., Walker, M., Wayth, R. B. 2019. The emission and scintillation properties of RRAT J2325-0530 at 154 MHz and 1.4 GHz. *Publications of the Astronomical Society of Australia* 36, e034. doi: 10.1017/pasa.2019.30
- Caleb, M., van Straten, W., Keane, E. F., Jameson, A., Bailes, M., Barr, E. D., Flynn, C., Ilie, C. D., Petroff, E., Rogers, A., Stappers, B. W., Venkatraman Krishnan, V., Weltevred, P. 2019. Polarization studies of rotating radio transients. *Monthly Notices of the Royal Astronomical Society* 487, 1191. doi: 10.1093/mnras/stz1352
- Burnham, K. P., Anderson, D.R. 2002. Model Selection and Multi-model Inference: A Practical Information-Theoretic Approach; Springer-Verlag New York, Inc.
- Timokhin, A. N. 2010. A model for nulling and mode changing in pulsars. *Monthly Notices of the Royal Astronomical Society* 408, L41. doi: 10.1111/j.1745-3933.2010.00924.x
- Yao, J. M., Manchester, R. N., Wang, N. 2017. A New Electron-density Model for Estimation of Pulsar and FRB Distances. *Astrophysical Journal* 835, 29. doi: 10.3847/1538-4357/835/1/29
- Malofeev, V. M., Smirnova, T. V., Soin, A. G., Shapovalova, N. V. 1995. Interstellar scintillation of pulsars at 102.7 MHz. *Astronomy Letters* 21, 619.